Food Biophysics (2020) 15:1–15
https://doi.org/10.1007/s11483-019-09596-w

ORIGINAL ARTICLE

Crystallization Kinetics and Mechanical Properties of Nougat Creme Model Fats

Stephen-Sven Hubbes[1] · André Braun[2] · Petra Foerst[3]

Received: 5 December 2018 / Accepted: 8 July 2019 / Published online: 15 July 2019

Abstract
Fat crystal networks result from a crystallization process, forming interlinked crystal aggregates of viscoelastic character. Palm oil-based fat crystal networks, such as chocolate and nougat spreads, often show liquid oil separation during storage because the fat crystal network is too weak to retain the liquid oils trapped within its structure. To explore the relationship between crystallization kinetics and subsequent mechanical properties, i) palm oil from three different geographical origins and with diverging crystallization properties, ii) mixtures of Ghanaian palm oil with gradually increasing additions of hazelnut oil, and iii) blends of Ecuadorian palm oil with palm stearin as a tripalmitin (PPP)-rich fraction were investigated. Kinetic parameters were acquired from an extended Avrami model by isothermal differential scanning calorimetry measurements, and the results combined with the elastic properties measured by oscillation rheology since studying crystallization kinetics alone insufficiently informs about the mechanical/structural properties needed to overcome liquid oil separation. Rate constants of all investigated fats followed bell-shaped curves, with curve progression strongly dependent on the lipid composition. Ameliorating crystallization properties entailed enhanced elastic properties. The higher the maximum rate constants, the higher the elastic modulus and the gel rigidity of the respective fats. However, two different linear regions of elastic modulus versus PPP or solid fat content resulted, depending on whether palm oil was diluted with hazelnut oil or blended with a PPP-rich fraction. Hazelnut oil strongly diluted crystallizable portions of the structuring fat, thereby decreasing the mechanical properties in a power-law fashion, because the fat crystal network became less connected between fat crystal aggregates.

Keywords Viscoelastic properties · Palm oil · Hazelnut oil · Crystallization kinetics · Avrami model · Oscillation rheology

Introduction

For the design of chocolate spreads and nut creams, good spreadability and a tender mouthfeel are key elements to meet consumer demands. To achieve this highly desirable semisolid texture, palm oil is often used. However, the use of palm oil may cause "oiling off" (liquid oil separation at the surface), due to its rather slow crystallization properties and tendency to produce soft fat crystal networks. This tendency is exacerbated by the addition of other liquid oils when producing nougat spreads, because of the proportion of liquid oil coming from, for example, nuts. All these characteristics can be attributed to the mechanical properties of the fat crystal network, which is a result of the previous crystallization process. Thus, influencing the crystallization properties of fat crystal networks with an understanding of the effect on the macroscopic properties is highly related to both shelf stability and sensory perception. For the food industry, this is of great interest, especially regarding palm oil-based products, such as nougat spreads, nut creams, and fillings. Additionally, this knowledge is of particular relevance to the organic food sector, as hydrogenation or interesterification of fats for modification of their plastic properties is not allowed by most organic food laws.

✉ Petra Foerst
petra.foerst@tum.de

[1] Rapunzel Naturkost GmbH, Rapunzelstr. 1, 87764 Legau, Germany

[2] Anton Paar Germany GmbH, Hellmuth-Hirth-Str. 6, 73760 Ostfildern-Scharnhausen, Germany

[3] Lehrstuhl für Systemverfahrenstechnik, Department of Food and Life Sciences, Technical University of Munich (TUM), Freising, Germany

A widely used method [1–5] to describe the crystallization kinetics and the dimensions of crystal build-up is the Avrami model (Eq. 1) [6]:

$$\Theta(t) = \frac{F(t)}{F(\infty)} = 1 - e^{(-kt^n)} \quad (1)$$

Where $\Theta(t)$ is the relative amount of crystallized fat at time t, $F(t)$ the absolute amount of crystallized fat at time t, and $F(\infty)$ the amount of crystallized fat at the very end of crystallization. The rate constant k comprises both the nucleation and growth rates and n is the Avrami exponent, which displays the dimension of crystal growth.

The original Avrami model was modified by Narine et al. [4], who provided a set of postulations regarding "crystallizing lipids and their nonadherence to the Avrami model," showing this nonadherence via distinct disruptions in the progression of the straight Avrami line in their Avrami plots. The authors solved this problem of nonadherence with one single and straight Avrami line, by regarding the crystallization of a lipid network as successional crystallization events, applying the Avrami model to each event separately. This extension to the original Avrami model has been corroborated and further explained by Hubbes, Danzl, and Foerst [7].

During the crystallization process of fats, crystals evolve, which then aggregate into flocs, forming a three-dimensional network of fractal structure, a colloidal gel. Shih et al. [8] derived a scaling theory for flocculated colloidal gels, which are very similar to fat crystal networks [9]. This scaling theory describes two different rheological regimes: i) the strong link regime at low solids volume fractions and ii) the weak link regime at high solids volume fractions. In the weak link regime, the stress at the limit of linearity, τ_0 (Pa), increases with increasing solids volume fraction Φ (= SFC/100 where SFC is the solid fat content), expressed in the following relation (Eq. 2) [8, 10]:

$$G\ddot{E} \sim \Phi^{1/(d-D)} \sim \tau_0 \quad (2)$$

Where D is the fractal dimension of the colloidal flocs arranged in d, the Euclidean dimension, with $d = 3$. The fractal dimension, D, is used to quantify the microstructure of the fat crystal networks [10–12]. Fat crystal networks have been proposed to be mostly in the weak link regime at SFC > 10% [13–15].

Though the Avrami model is solely a kinetic model, not giving a direct conclusion on the final structure of the fat crystal network, the pathway by which a fat crystallizes and forms a unique three-dimensional network is related to its resultant mechanical properties [14, 16–18]. Rheologically, the stress at the limit of linearity τ_0, is the point, above which, interfloc links between the fat crystal aggregates, first begin to break. Consequently, τ_0 can be seen as an indicator of the resilience of the fat crystal network, not only against applied force but also against "oiling off": when the network breaks, it loses its capacity to retain the liquid oils trapped within its network.

Despite the works mentioned above that indicate a general relationship between crystallization and mechanical properties [14, 16–18], this process is still not fully understood. Despite newer works [19–21] showing that the mechanical properties of fats diluted with liquid oil are generally linked with the crystallization kinetics, deeper investigations into the crystallization properties and their effect on subsequent structural properties, especially for nougat cremes, is left open to further exploration. Even though hardness (G') of palm oil-based fats and the fractal dimension of cocoa butter could be related to the Avrami exponent [16, 17], rate constants (k) and their influence on the resulting mechanical properties, including the stress at the limit of linearity associated with "oiling off", were scarcely analyzed.

Our study resumes these investigations, by combining the Avrami model in its extended version [4, 7] with oscillation rheology experiments, to determine how rate constants (k) and Avrami exponents (n) coincide with the solids volume fraction (Φ), the elastic modulus (G'), the stress at the limit of linearity (τ_0), and the gel rigidity (m). For this purpose, three distinct origins of palm oil, exhibiting differences in their crystallization behavior, due to variations in their lipid composition, were the basis to modify the crystallization properties further. Thus, i) a palm oil with slow crystallization properties was enriched with palm stearin as a tripalmitin (PPP)-rich fraction, and ii) a palm oil with fast crystallization properties was diluted with hazelnut oil, to explore the physical effects of fat types commonly used in the confectionery sector on crystallization kinetics and mechanical properties of the fat crystal network. Hence, this study investigates how either crystallization promoters via PPP or liquid oil coming from hazelnuts modifies the mechanical response of a fat crystal network and how previous crystallization kinetics, the solid fat content via Φ, and the subsequent mechanical properties are interrelated.

From a practical perspective, more understanding is generated on how hazelnut oil affects the structural and kinetic properties of nougat cremes, and how crystallization and elastic properties of the underlying fat crystal network could be improved to generate nougat cremes with optimum properties to meet consumer demands.

Materials and Methods

Experimental conditions were chosen to study the background of network formation during production of nougat cremes. Therefore, isothermal crystallization studies have been conducted with temperatures at which phase transitions from

liquid to solid occur. Oscillation rheometry was utilized to investigate the nature of such fat crystal networks in a post-crystallization state. To better correlate results from the crystallization studies with the structural properties measured by oscillation rheometry, the investigations were complemented by SFC measurements. Table 1 shows the test setup, with the different oil blends and the chosen parameters for oscillation rheology and crystallization studies.

Materials

Three different origins (Ghana, Colombia, and Ecuador) of refined, bleached, and deodorized palm oil; the hard fraction of a single-fractionated palm oil (trade name "palm stearin"); and hazelnut oil obtained from roasted, ground hazelnuts (all ingredients with organic status, based on EU Regulation 834/2007) were provided by Rapunzel Naturkost GmbH (Legau, Germany).

As Ecuadorian palm oil had the lowest PPP content, it was selectively enriched with palm stearin, to investigate the influence on the crystallization kinetics and mechanical properties. Palm oil from Ghana, which showed the fastest crystallization among the investigated origins, was diluted with hazelnut oil in 10% (*w*/w) increments. Differential scanning calorimetry (DSC) studies were conducted for mixtures with 20, 40, 50, and 60% hazelnut oil mixed with Ghanaian palm oil. Table 1 shows the test setup.

Hazelnut Oil Extraction

Freshly roasted and ground hazelnuts were left undisturbed, to allow the nut particles to sediment. The oil layer that formed at the surface of the hazelnut paste was decanted, centrifuged (Allegra X-15, Beckman Coulter, Inc., Brea, CA, USA) at 4750 rpm for 180 min and then decanted again, to obtain a blank oil, free from any residual nut particles.

Table 1 The experimental setup and the differant fat samples (with their respective Tripalmitin content) used for oscillation rheology and the isothermal DSC studies for the investigation of structural properties and crystallization kinetics

	Fat samples		Oscillation Rheology			DSC studies used for the Avrami model
		Tripalmitin content [%]	stress sweeps [Pa]; f = 1 Hz	Applied normal force, F [N]	frequency sweeps [Hz]	Isothermal crystallization temperature $T_{isotherm}$ [°C]
Geographical origins of palm oil						
A	Ecuador, 100%	6.75 (± 0.13)	1–12000	10	0.1–100	16 18 19 19.5 20 20.5 21 21.5 22 23 24
B	Ghana, 100%	7.17 (± 0.36)	1–12000	10	0.1–100	16 18 19 19.5 20 20.5 21 21.5 22 23 24
C	Colombia, 100%	7.98 (± 0.23)	1–12000	10	0.1–100	16 18 19 19.5 20 20.5 21 21.5 22 23 24
Blends of Ecuadorian palm oil with palm stearin (PS)						
A-1	95% + 5% PS	7.45 (± 0.13)	1–15000	10	0.1–100	16 18 19 19.5 20 20.5 21 21.5 22 23 24 25 26
A-2	90% + 10% PS	8.15 (± 0.14)	1–15000	10	0.1–100	16 18 19 19.5 20 20.5 21 21.5 22 23 24 25 26 27
A-3	80% + 20% PS	9.54 (± 0.15)	1–15000	10	0.1–100	19 20 21 22 23 24 24.5 25 25.5 26 27 28
Blends of Ghanaian palm oil with hazelnut oil (HO)						
B-1	90% + 10% HO	6.45 (± 0.29)	1–12000	10	0.1–100	
B-2	80% + 20% HO	5.73 (± 0.25)	1–6000	10	0.1–100	16 17 18 19 19.5 20 20.5 21 22
B-3	70% + 30% HO	5.02(± 0.22)	1–3000	1	0.1–100	
B-4	60% + 40% HO	4.30 (± 0.19)	0.1–1000	1	0.05–50	12 14 16 16.5 17 17.5 18 19 20
B-5	50% + 50% HO	3.58 (± 0.16)	0.01–1000	0.2	0.02–20	12 13 14 15 16 17 18 19
B-6	40% + 60% HO	2.87 (± 0.13)	0.01–1000	0.2	0.02–20	8 9 10 11 12 13 14 15 16

All the origins of palm oil and all the blends have been studied with triplicate measures for the DSC studies and quintuplicate measures for the rheological studies. Values in parenthesis represent confidence intervals ($\alpha = 0.05$) for the different origins of palm oil and calculated measurement failure for the blends

Preparation of Samples

For the respective blends, palm oil, palm stearin, and hazelnut oil were heated to 80 °C and thoroughly mixed after weighing the respective amounts, according to Table 1. Once prepared, the bulk samples were stored frozen (−18 °C).

Methods

Crystallization Kinetics

For the kinetic data, isothermal crystallization measurements were performed on a Netzsch Maia F3 200 DSC (Selb, Germany) device. Samples of the molten (60 °C) blends (10–20 mg) were placed in aluminum pans, which were hermetically sealed and inserted into the DSC, along with an empty aluminum pan as a reference. Samples were heated to 60 °C (10 °C/min) for 8 min to erase all crystal memory and then rapidly cooled (20 °C/min) to the isothermal condition, which was held for 60 min, to obtain the crystallization curves. For the extended Avrami model, the data from the DSC crystallization curves were integrated and applied in the Avrami plot, by logarithmic function based on Eq. (1). The original Avrami equation (Eq. 1) was applied to each mode of crystallization in the following way (Eq. 3):

$$\frac{F_i(t)}{F_i(\infty)} = 1 - e^{\left[-k_i(t-\tau_i)^{n_i}\right]}, \quad \text{for } t > \tau\text{i} \tag{3}$$

Where each crystallization mode i is characterized by a single absolute crystallinity $F_i(t)$ at time t, and τ_i, the incubation time after each mode would begin. $F_i(\infty)$ is the total crystallinity for the ith event, finally resulting in Eq. (4):

$$F(t) = \Sigma_{i=1}^{N} F_i(t) \tag{4}$$

When the i crystallization growth modes are summed; thus, every growth mode shows its associated rate constant k and dimension of crystal growth n, as originally presented by Narine et al. [4]. A detailed description of this procedure and how to employ crystallization curves to the extended Avrami model is provided in the literature [7].

The rate constants of each different growth mode (Eq. 3) were summed by applying the above procedure, forming the global rate constant k_g, and characterizing the overall crystallization rate, as shown in Eq. (5):

$$k_g = \Sigma_{i=1}^{N} k_i \tag{5}$$

Where k_g is the global rate constant, including nucleation and crystal growth of all the segments, and N is the total number of segments or different growth modes, respectively. The global rate constant k_g gives the arithmetic mean, enabling the comparison of the overall crystallization properties of different fats under a variety of different isothermal conditions. This procedure was utilized for examining the crystallization kinetics of all the blends investigated in this study.

When viewing the isothermal DSC crystallization curves, their progression typically begins with an onset, followed by a maximum (crystallization peak) recorded by the DSC, with the DSC signal then decaying to baseline level. These characteristic steps in the curve progression of the crystallization process (onset, peak, and return to baseline level) were associated with different growth modes of fat crystals [7]. Since every growth mode had its distinct Avrami exponent, the exponent from the crystallization peak was chosen as the signal recorded in the DSC and, thus, the crystallization reaction was maximized at this stage. Furthermore, Avrami exponents at $k_g\,max$ were taken as reference points to improve the correlation of crystal growth dimension with the resultant mechanical properties, and are further denoted as n, for comprehensibility reasons.

The thermodynamic driving force of the transition from liquid oil to solid fat is represented by the chemical potential difference $\Delta\mu_i$ between the ith crystallized triglyceride (TG) species in the solid state and the ith TG species in solution in the melt (see Eq. 6).

$$\Delta\mu_i = \Delta H_{m,i}\left(T_{m,i} - T\right)/T_{m,i} \tag{6}$$

Where $\Delta H_{m,\,i}$ is the melting enthalpy (J/mol) of the ith TG moiety from a neat state, $T_{m,\,i}$ is the melting temperature (K) of the ith TG moiety, and T is the temperature (K) of isothermal crystallization. Hence, $(T_{m,\,i} - T)$ represents the degree of supercooling of the ith TG moiety [1, 22]. Therefore, a lower crystallization temperature leads to a higher degree of supercooling.

DSC Heating Thermograms

DSC heating thermograms were acquired to record how different fat compositions affect the melting profiles of the investigated palm oils and their mixtures. Therefore, samples were heated at a rate of 5 K/min directly after isothermal crystallization had been terminated (see section 2.2.1). All DSC analyses were carried out in triplicate.

High-Performance Liquid Chromatography (HPLC) of TGs

The diglycerides and TGs in the palm oils of different geographical origins, the palm stearin and the hazelnut oil were chromatographically separated on a Nucleosil 120–3 ET C18 column (250 × 4.0 mm; Macherey-Nagel GmbH & Co. KG, Düren, Germany) protected by a SecurityGuard™ C18 pre-column

(4 × 3.0 mm; Phenomenex, Inc., Aschaffenburg, Germany). Acetonitrile–ethyl acetate (50/50 *v*/v) served as the mobile phase, and a Sedex 85 evaporative light scattering detector (Sedere SA, Alfortville Cedex, France) was implemented. The different TGs were quantified by HPLC analysis using Chromeleon software (Thermo Fisher Scientific, Waltham, MA, USA) and cocoa butter as the standard. Values of PPP were determined for the palm oils of different geographic origins, palm stearin, and hazelnut oil. Values of PPP for the blends were then calculated, and, also, the measuring error. Samples were analyzed in triplicate.

Oscillation Rheology

Rheological measurements were performed using an MCR502 rheometer (Anton Paar, Ostfildern, Germany). Sandblasted parallel plates (PP-25) of 25 mm in diameter were used to avoid wall slippage of the samples. A Peltier P-PTD200/80/I element, together with a Peltier H-PTD200 hood, was used to prevent temperature gradients between the upper and lower plates and for maintaining a constant measurement temperature.

To prepare the samples, pellets of fat were produced by pouring molten palm oil into precooled Teflon molds of 25 mm in diameter and 2.2 mm thickness. An even distribution of the palm oil in the molds was ensured to avoid uneven surfaces resulting from contraction of the hardening fat upon its crystallization. The temperature protocol for crystallization and subsequent storage was similar to that used in the industrial production of chocolate spreads and nougat spreads, which involves (1) filling the molten dispersion into jars, (2) cooling them in a cooling tunnel, and (3) transferring them to the warehouse for further solidification. Accordingly, the filled molds were set to crystallize in a cooled (10 °C) and ventilated room for 20 min and were then transferred to a controlled atmosphere and held at 20 °C for 24 h for the equilibration of G' before the actual measurements. A measurement temperature of 20 °C was chosen, as this approximates the consumption temperature of nougat spreads by consumers.

In order to preserve its native structure when transferring the fat pellet into the rheometer gap, samples were frozen at −18 °C, for complete hardening. As fats further contract upon deep freezing, they could be gently pushed out of the molds into the rheometer gap. An adjustment time of 5 min was granted before preparing for measurements. A normal force (F_N) was set (see Table 1) and kept constant during measurements to avoid wall slip, whereas, a rather low F_N was used to avoid breakage of the samples with higher portions of hazelnut oil.

To define the linear viscoelastic region (LVR) of the palm oils and palm oil blends, stress sweeps were applied to all samples listed in Table 1, at a constant frequency of 1 Hz. The stress at the limit of linearity τ_0 was determined as the yield point, beginning with a 5% deviation from the LVR line. Frequency sweeps at a constant stress $<\tau_0$ were performed for obtaining the gel rigidity, m. The utilized frequency was applied according to Table 1. Results from rheological measurements were the means of five runs.

As described by Mezger [23], the slope m of the function $G'(f)$ is known to be the progressively growing resistance of the network structure against faster movements, due to a certain degree of rigidity. As a result, m can be defined as an indicator of gel rigidity and thereby an indicator of spreadability.

SFC

To measure the SFC, low-resolution nuclear magnetic resonance (NMR) was performed using a Bruker Minispec MQ20 (Bruker BioSpin GmbH, Rheinstetten, Germany). First, the different palm oils and blends were molten under stirring at 65 °C and then cast into NMR test tubes up to a level of 4 cm. The NMR test tubes were put in precooled aluminum sample holders, set to crystallize in a refrigerator and then transferred to a temperature condition of 20 °C for 24 h, analogous to the fat pellets for oscillation rheology. Before analysis, the samples were placed in a tempered water bath for at least 30 min, to adjust to the respective measurement temperature and then transferred to the tempered NMR, for obtaining the SFC via the direct method [24]. Samples were measured in triplicate.

Statistical Methods

One-way analysis of variance was performed, followed by the Holm–Sidak post hoc test with a significance level of $\alpha = 0.05$ to compare τ_0 and G', the different PPP contents, k_g *max*, n, and Φ of the palm oils of different geographic origins and their blends. Linear regression was applied to describe the relationship between i) k_g *max* and the PPP content, ii) log G' with log Φ, and iii) the gel rigidity m and τ_0 with the PPP content of the samples. Pearson's correlation was used to demonstrate the strength of the interaction between crystal growth dimension n with the elastic modulus G'. Statistical analysis, including a normality test (Shapiro–Wilk) and a constant variance test, was performed using SigmaPlot version 12 (Systat Software, Inc., San Jose, CA, USA).

Results and Discussion

Lipid Profile of Palm Oils of Different Geographic Origins, Palm Stearin, and Hazelnut Oil

The dominant fatty acids present in the TGs of the investigated fats were palmitic acid (P; "Saturated (Sat)-type"), stearic acid (S; "Sat-type"), oleic acid (O; "Unsaturated (U)-type"), and linoleic acid (L; "U-type"). The dominant TGs of the respective fats were clustered together by their fatty acid type (e.g., U-U-U-type TG, Sat-U-U-type TG). The dominant fully

saturated TG was PPP, and triolein (OOO) was the dominant unsaturated TG of palm oil, palm stearin, and hazelnut oil, alike. These results are comprehensively shown in Table 2 and correspond well with the literature [25–27].

Crystallization Kinetics of Palm Oils of Different Geographic Origins and their Blends with Palm Stearin and Hazelnut Oil, Based on the Extended Avrami Model

Global rate constants, k_g, were formed according to Eq. (5) and plotted as a function of temperature (see Fig. 1) for the palm oils of different geographic origins (Fig. 1b), the blends of Ghanaian palm oil with hazelnut oil (Fig. 1a), and the blends of Ecuadorian palm oil with palm stearin (Fig. 1c). The progression of k_g for all the blends followed a bell-shaped character, typically described for overall crystallization processes. Large differences in the peak values ($k_g\,max$) and the course of the progression of the bell-shaped curves of k_g were observed for the different blends of palm oil and the mixtures of hazelnut oil.

It is generally known that palm oil is comprised of many different TGs, which can be separated into fractions, most commonly known as a lower melting "olein"

Table 2 Comparison of triglycerides and diglycerides from different origins of palm oil, palm stearin and hazelnut oil. Triglycerides clustered together in groups: "U"=unsaturated fatty acid chain; "Sat"=saturated fatty acid chain

Fat composition		Origin of palm oil			Palm stearin	Hazelnut oil
		Ecuador	Ghana	Colombia		
Triglycerides (TG, %)						
U-U-U-type TG	LLL	n.d.	n.d.	n.d.	n.d.	1.65 (± 0.06)
	LLO	1.56 (± 0.12)	n.d.	n.d.	n.d.	4.44 (± 0.05)
	LOO	3.70 (± 0.06)	3.26 (± 0.21)	3.25 (± 0.05)	1.19 (± 0.06)	15.57 (± 0.09)
	OOO	6.37 (± 0.05)	5.71 (± 0.33)	6.05 (± 0.09)	3.14 (± 0.21)	51.35 (± 0.17)
Sat-U-U-type TG	PLO	11.11 (± 0.02)	10.61 (± 0.57)	10.78 (± 0.25)	5.16 (± 0.14)	4.32 (± 0.07)
	PLL	4.03 (± 0.12)	3.52 (± 0.19)	3.28 (± 0.08)	n.d.	1.31 (± 0.02)
	POO	19.48 (± 0.11)	18.87 (± 1.00)	20.21 (± 0.62)	15.67 (± 0.95)	14.49 (± 0.1)
	SOO	4.17 (± 0.04)	3.89 (± 0.19)	3.47 (± 0.10)	1.84 (± 0.07)	5.4 (± 0.04)
Sat-U-Sat-type TG	POP	21.33 (± 0.08)	22.29 (± 1.02)	23.6 (± 0.71)	28.81 (± 0.99)	1.47 (± 0.14)
	PLP	10.04 (± 0.03)	9.74 (± 0.51)	10.07 (± 0.26)	5.85 (± 0.38)	n.d.
	POS	7.06 (± 0.13)	6.95 (± 0.25)	6.35 (± 0.16)	5.67 (± 0.39)	n.d.
	SOS	n.d.	n.d.	n.d.	0.95 (± 0.08)	n.d.
Sat-Sat-Sat-type TG	PPP	6.75 (± 0.11)	7.17 (± 0.32)	7.98 (± 0.20)	20.7 (± 0.02)	n.d.
	PPS	2.03 (± 0.16)	2.04 (± 0.2)	2.07 (± 0.13)	4.17 (± 0.41)	n.d.
Diglycerides	(%)	6.28[b] (± 0.20)	5.94[b] (± 0.07)	7.01[b] (± 0.02)	4.7 (± 0.11)	< 1.0
U-U-U-type TG		11.59[b] (± 0.23)	8.97[a,b] (± 0.54)	9.30[a,b] (± 0.14)	4.33 (± 0.27)	73.01 (± 0.37)
Sat-U-U-type TG		38.79[a] (± 0.29)	36.89[a] (± 1.95)	37.74[a] (± 1.05)	22.67 (± 1.16)	25.52 (± 0.23)
Sat-U-Sat-type TG		38.43[a] (± 0.26)	38.98[a] (± 1.78)	40.65[a] (± 1.13)	41.28 (± 1.84)	1.47 (± 0.14)
Sat-Sat-Sat-type TG		8.78[a] (± 0.27)	9.21[a] (± 0.52)	10.05[b] (± 0.33)	24.87 (± 0.43)	n.d.

[a] no statistically significant difference

[b] statistically significant difference

Measured by HPLC analysis with standard deviation given in parenthesis from triplicate measurements

n.d. not detectable

and a higher melting "stearin." The olein fraction corresponds to U-U-U-, Sat-U-U-, and Sat-U-Sat-type TGs. The stearin fraction consists mostly of Sat-U-Sat- and Sat-Sat-Sat-type TGs [7, 25, 26]. Coming from the right-hand side of the curves of k_g (see Fig. 1b), the supercooling is lower, as the temperature difference between the melt temperature and isothermal crystallization temperature ($T_{isotherm}$) is relatively small. Hence, the high melting fractions of the palm oils firstly crystallize from the melt because their chemical potential difference $\Delta\mu_{HM}$ (where *HM* denotes high melting; see Eq. 6) is higher compared with the lower melting fractions. Consequently, the higher isothermal region (right-hand side of the curve) is characterized by less nucleation, due to lower supercooling, which leads to reduced rate constants. When supercooling is increased, more of the lower melting TGs are crystallized, with more nuclei being generated, ultimately growing into crystals. This process accelerates the crystallization process to a certain maximum, k_g *max* [7]. If the degree of supercooling is further increased, faster crystallization would be expected, but the opposite occurs, as Fig. 1a–c shows. This behavior is a general observation for all the oil blends in this study. The decreasing global rate constants beyond k_g *max* (left-hand side of the curves) can be attributed to a growing diffusion barrier, as viscosity is increased by the lower melt temperature and by the abundance of crystallizing TGs competing for the same crystallization sites [7, 28, 29].

As the rate constant of the Avrami model is a composite constant, including both nucleation rate and crystal growth [1, 6, 30], an optimum between a high nucleation rate and a fast diffusion of molecules to the sites of crystallization must be present at the maximum rate constant, k_g *max*. These effects on palm oil have already been extensively discussed [7] and are now also shown for palm oils diluted with hazelnut oil (Fig. 1a).

Palm Oils of Different Geographic Origins

Earlier work [7] reported that the different rate constants of the different origins of palm oil were primarily attributable to their PPP/OOO ratios. The Ecuadorian palm oil had the lowest PPP/OOO, rate constant k_g, and maximum rate constant k_g *max*, among those of different geographic origins. No significant difference existed between the PPP/OOO ratios of the Colombian and Ghanaian palm oils, whereas, the Colombian palm oil had the significantly highest diglyceride levels (see Table 2). Diglycerides are known to influence nucleation and crystallization speed [31], thereby explaining the slightly decreased maximum rate constants of Colombian palm oil compared with Ghanaian palm oil.

Palm Oil Diluted with Hazelnut Oil

The dilution of palm oil with hazelnut oil is accompanied by a noticeable reduction in the quantity of tri- and di-saturated fats (Sat-Sat-Sat- and Sat-U-Sat-type TGs), notably PPP and POP (see Tables 1 and 2), the higher the addition of hazelnut oil. Therefore, an increase in the amount of TG, consisting especially of tri-unsaturated fatty acids (U-U-U-type TG), particularly OOO, occurs by gradually increasing the amount of hazelnut oil (see Table 2 for an indication). To exemplify, adding 20% hazelnut oil leads to a reduction of Sat-U-Sat-type TGs from 38.98 to 31.48%, accounting for 81% of the original value found in the Ghanaian palm oil.

When Ghanaian palm oil (Fat B) was diluted with hazelnut oil, k_g *max* was reduced in relation to the gradually increasing hazelnut oil addition. Additionally, with an increasing amount of hazelnut oil added, the profile of the bell-shaped curves of the rate constants flattened when compared with the undiluted Ghanaian palm oil, Fat B (see both in Fig. 1a). Some investigations [19–21] have shown the inhibiting influence of liquid oils on palm oil crystallization, attributing the inhibitory effect mainly to the abundance of unsaturated fatty acids, yet these authors did not further specify which fraction of crystallizing palm oil is most affected upon dilution with liquid oils.

As Fig. 2 shows in the blends, gradually replacing palm oil with increasing addition of hazelnut oil, leads to an overproportionate reduction in the melting enthalpy (ΔH_m) of the peak associated with the olein fraction. ΔH_m associated with the Sat-U-Sat-type TG decreases more drastically (from 22.23 to 12.53 J/g, which is 56% of the value of the undiluted Ghanaian palm oil) compared with the drop to 81% of the original value of Sat-U-Sat-type TG. The disproportionate drop in ΔH_m is exacerbated when more hazelnut oil is added, until the point where the peak associated with the olein fraction almost disappears (namely, upon a dilution with 60% hazelnut oil; see Fig. 2). In comparison, ΔH_m of the stearin peak decreases in a more proportional manner, commensurable to the hazelnut oil addition (data not shown; see Fig. 2 for an indication). Therefore, hazelnut oil preferentially solubilizes POP in the blends since the olein peak of the DSC curves is most affiliated with POP [7, 25, 26].

Lipids exhibit both melt and solution behaviors [32]. As the olein peak contributes the most to the overall melting enthalpy ΔH_m of palm oil (see Fig. 2), its overproportionate reduction induced by gradually increasing hazelnut oil addition would, therefore, significantly decrease the chemical potential difference $\Delta\mu_i$ (see Eq. 6) [1]. Consequently, to overcome the activation free energy for the formation of stable nuclei, supercooling must be increased (see Eq. 6). Moreover, by increasing supercooling, additional TGs may crystallize from the melt because their solubility in the hazelnut oil, acting as a

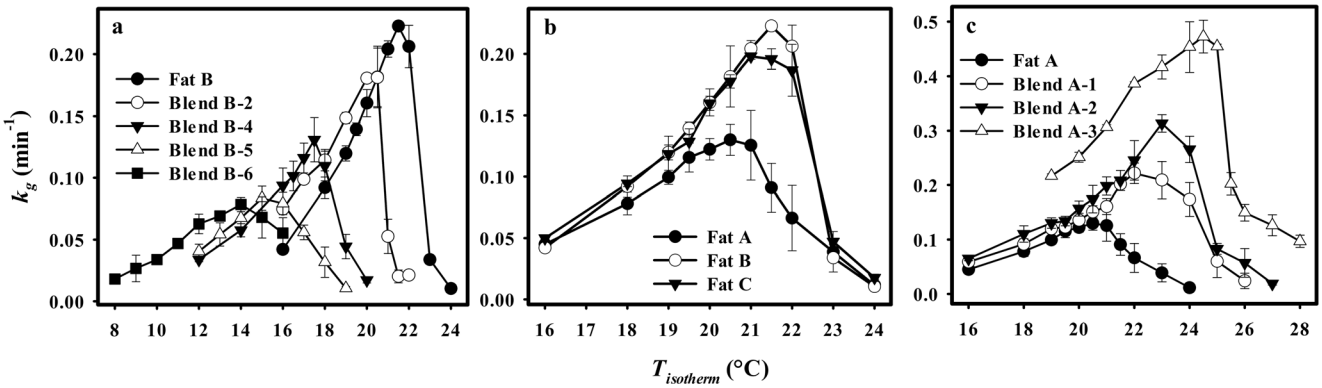

Fig. 1 **a** Rate constants k_g of Ghanaian palm oil (Fat **B**) and its dilutions with increasing amounts of hazelnut oil (HO) (**B-2**: 20% HO; **B-4**: 40% HO; **B-5**: 50% HO; **B-6**: 60% HO); **b** k_g of palm oils of three different geographical origins (Fat **A**: Ecuador; Fat **B**: Ghana; Fat **C**: Colombia), and **c** k_g of Ecuadorian palm oil (Fat **A**) and its blends with increasing amount of palm stearin (PS) as a PPP-rich fraction (**A-1**: 5% PS; **A-2**: 10% PS; **A-3**: 20% PS). Graphs from (b) and (c) taken from [7]. Error bars represent the confidence intervals ($\alpha = 0.05$) from triplicate measures

solvent, has been decreased with lower temperatures [32]. This phenomenon is demonstrated by the shift in the bell-shaped course of k_g and their peak maxima, k_g *max*, toward lower crystallization temperatures, the higher the amount of hazelnut oil replacing palm oil (see Fig. 1a).

An additional reason for the overproportionate decrease in ΔH_m is the reduction in the percentage of PPP by the increasing hazelnut oil addition (see Tables 1 and 2). PPP forms mixed crystals with POP, thereby leading to a better seeding of the crystallization process and increased crystallization rates [33–35]. Moreover, de Oliveira et al. [5] stated that PPP promotes crystal growth, as it allows more material to accumulate in the same isothermal range by acting as templates in the crystal lattice ordering process. Accordingly, having lower levels of PPP by replacing palm oil with hazelnut oil, less POP is co-crystallizing, further explaining the observed drop in ΔH_m (Fig. 2), also, reflected in a decreasing k_g *max* as a function of PPP, as in Fig. 3.

Palm Oil with Palm Stearin Added

As large fractions of TG in the palm oil diluted with hazelnut oil (blends of the B-series) remain solubilized during the crystallization triggered by increasing hazelnut oil contents, k_g *max* drops in accordance with the increase of hazelnut oil (see Fig. 3). When adding increasing amounts of a PPP-rich fraction to Ecuadorian palm oil showing slower crystallization properties (Fat A and blends of the A-series), the rate constants sharply increase with the addition of the PPP-rich fraction which is reflected in the observation of two different linear regions of maximum rate constants k_g *max,* in Fig. 3.

The presence of two linear regions with different slopes is not surprising because increasing contents of PPP enhance the melting enthalpy $\Delta H_{m,\,i}$, not only by having more PPP present in the melt but, also, due to an enhanced co-crystallization of TGs from the olein fraction, as could be seen in our DSC melting curves (data not shown). The observation is consistent

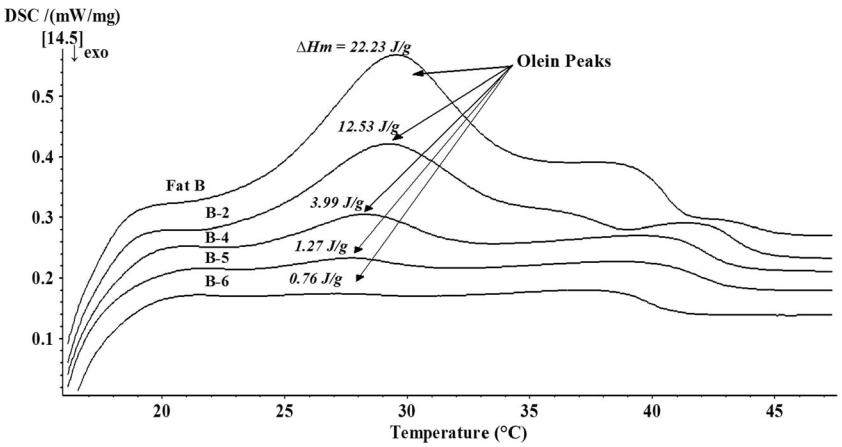

Fig. 2 Dilution effect of hazelnut oil (HO) on the olein fraction of Ghanaian palm oil (Fat **B**) is shown, in particular, in this exemplified presentation of the differential scanning calorimetry (DSC) heating thermograms. ΔH_m signifies the melting enthalpy (J/g) of olein peaks of the respective dilutions (from triplicate measures; no confidence intervals due to clarity reasons). Fat **B-2**: 20% HO; **B-4**: 40% HO; **B-5**: 50% HO; **B-6**: 60% HO. All oils were pre-crystallized isothermally at 16 °C for 60 min and melted at 5 K/min, measured in triplicate, to obtain the DSC heating thermograms

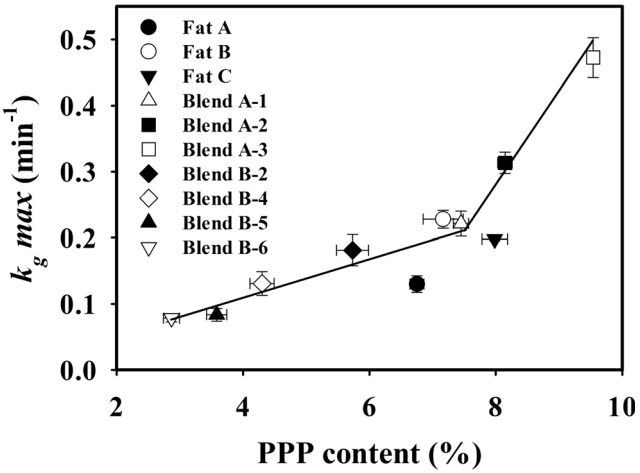

Fig. 3 Maximum rate constants k_g *max* plotted as a function of the tripalmitin (PPP) content of the palm oils of different geographic origins, Ghanaian palm oil and its dilutions with hazelnut oil (HO), and Ecuadorian palm oil blended with palm stearin (PS) as a PPP-rich fraction. Fat **A**: Ecuador; **B**: Ghana; **C**: Colombia, **A-1**: 5% PS; **A-2**: 10% PS; **A-3**: 20% PS, **B-1**:10% HO, **B-2**: 20% HO; **B-3**: 30% HO; **B-4**: 40% HO; **B-5**: 50% HO; **B-6**: 60% HO. Confidence intervals ($\alpha = 0.05$) from triplicate measures

with the literature [5, 33–35] that shows improved seeding and co-crystallization of POP in the presence of enhanced levels of PPP. This effect is becoming most apparent when comparing the profile of the curve of k_g for Ghanaian palm oil mixed with 60% hazelnut oil with that of the Ecuadorian palm oil mixed with 20% palm stearin. Both mixtures are diametrically opposed to each other regarding their PPP content (see Tables 1 and 3) and the profile of their curves of k_g (see Fig. 1a, c, in particular).

Elastic Properties of the Fat Crystal Network in Relation to the PPP Content and the Solids Volume Fraction Φ of the Blends

When a fat crystallizes, its fat crystals aggregate and grow into clusters/flocs, which are connected by interfloc links, forming a colloidal gel. The elastic properties of such a network depend on the number of connections between neighboring structural clusters [36]. Generally, as the relationship between τ_0 and Φ in Fig. 4 indicates, the fats are in the weak link regime for all the investigated samples [8, 10], meaning that the fat crystal aggregates are connected to each other by interfloc links.

According to expectation, the elastic properties of palm oil are lowered by the addition of hazelnut oil and increased with the addition of a PPP-rich fraction. However, two different linear regions of mechanical response can be identified in Fig. 4, depending on whether the palm oil was diluted with hazelnut oil or blended with palm stearin (including the three different geographic origins).

The different linear regions of mechanical response for different plant oils were first shown by Awad et al. [10] and further discussed by other investigators [12, 36, 37]. In this study, two different linear regions for the mechanical response are also shown for palm oil diluted with hazelnut and mixed with palm stearin. Awad et al. [10] yielded a straight line with slope μ when plotting G' versus Φ in log-log plots. The slope can then be used to calculate the fractal dimension D [11; Eq. 7], which can be inserted into Eq. (2) to calculate G':

$$D = 3 - \frac{1}{\mu} \tag{7}$$

Hence, the different linear regions of the mechanical responses observed in Fig. 4 are related to different fractal growth dimensions of palm oil diluted with hazelnut oil versus palm oil blended with palm stearin.

Values of log G', increase faster in the low SFC region (4.7–15.9% SFC), corresponding to the blends with hazelnut oil (B-series), as can be seen by their steeper slope (see Fig. 4a), and then increase more slowly in the higher SFC region (20.4–34.0% SFC); corresponding to the palm oils of different geographic origins and the blends with a PPP-rich fraction. The transient point for the two different linear regions of mechanical response is located around Fat B-2 (see Fig. 4), which is consistent with the previous observation of two different linear regions of maximum rate constants k_g *max*, shown in Fig. 3. From a design perspective, in a colloidal network, the system is composed of interconnected structural clusters separated by hollow spaces [8]. The hollow space of the largest size in a region represents a kind of "flaw" and becomes a stress concentrator in that area. Additionally, there are always differences between neighboring fat crystal flocs, and so the strength of the interfloc links is different. The weakest floc will become a flaw and will, thus, act as a stress concentrator [12]. The elastic properties of the whole network are dominated by the elastic strength of these stress concentrators [9]. Hence, stress is distributed heterogeneously on the interfloc links and held by a specific stress-carrying volume fraction of solids [37]. As shown in section 3.2.2, Hazelnut oil strongly solubilizes bulk crystallizable portions of palm oil. As a consequence, hazelnut oil introduced into palm oil (i) reduces the connectivity of the network, (ii) creates more and larger hollow areas and results in (iii) having weaker interfloc links. Hence, the stress-carrying solids decrease dramatically, the more hazelnut oil is added. In turn, there is a greater reduction in the mechanical properties, shown by the steeper slopes of log G', log τ_0, and m with the SFC in the low SFC region [10, 12, 38], as comprehensively shown in Fig. 4. Moreover, the combined effects of (i)—(iii) explain why the point of inflection between the

Table 3 Comprehensive data of the palm oils of different geographic origins and their blends with either palm stearin or hazelnut oil

				PPP content [%]	k_g *max* [min^{-1}]	Avrami exponent *n*	τ_0 [Pa]	G´ *E+06 [Pa]	degree of rigidity, *m* * E+04 [Pa/Hz]	*Φ* [SFC/100]
Higher SFC region	Origins of palm oil	A	Ecuador, 100%	6.75 (± 0.13)	0.130^{d} (± 0.013)	$3.6^{g, j}$ (± 0.2)	401 (± 35)	4.00 (± 0.36)	14.16 (± 0.61)	0.228 (± 0.001)
		B	Ghana, 100%	7.17 (± 0.36)	0.228^{c} (± 0.013)	$4.1^{h, l}$ (± 0.2)	559^{a} (± 44)	5.60 (± 0.43)	23.41 (± 2.23)	0.2529 (± 0.000)
		C	Colombia, 100%	7.98 (± 0.23)	0.198^{c} (± 0.002)	$4.0^{h, l}$ (± 0.1)	588^{a} (± 31)	5.86 (± 0.30)	20.09 (± 0.1)	0.281^{f} (± 0.001)
	Blends of Ecuadorian palm oil with palm stearin	A-1	95% + 5% PS	7.45 (± 0.13)	0.221^{c} (± 0.019)	$4.1i^{h, l}$ (± 0.1)	535^{a} (± 22)	5.35 (± 0.23)	17.22 (± 0.79)	0.234 (± 0.003)
		A-2	90% + 10% PS	8.15 (± 0.14)	0.313 (± 0.016)	4.3^{h} (± 0.0)	675 (± 34)	6.72 (± 0.38)	20.89 (± 0.9)	0.283^{f} (± 0.002)
		A-3	80% + 20% PS	9.54 (± 0.15)	0.472 (± 0.030)	$3.9^{g, l}$ (± 0.0)	829 (± 17)	8.28 (± 0.18)	26.39 (± 0.4)	0.340 (± 0.002)
Lower SFC region	Blends of Ghanaian palm oil with hazelnut oil	B-1	90% + 10% HO	6.45 (± 0.29)	n.a.	n.a.	318 (± 17)	3.18 (± 0.17)	15.07 (± 0.15)	0.204 (± 0.001)
		B-2	80% + 20% HO	5.73 (± 0.25)	0.181 (± 0.024)	$3.4^{j, k}$ (± 0.2)	209 (± 1.2)	2.09 (± 0.09)	10.11 (± 0.44)	0.159 (± 0.001)
		B-3	70% + 30% HO	5.02 (± 0.22)	n.a.	n.a.	26.5 (± 1.2)	0.528 (± 0.02)	2.54 (± 0.19)	0.118 (± 0.002)
		B-4	60% + 40% HO	4.30 (± 0.19)	0.131^{d} (± 0.018)	3.2^{k} (± 0.0)	10.7^{b} (± 0.6)	0.213 (± 0.01)	1.11 (± 0.01)	0.084 (± 0.001)
		B-5	50% + 50% HO	3.58 (± 0.16)	0.084^{e} (± 0.010)	2.7^{i} (± 0.1)	3.1^{b} (± 0.2)	0.030 (± 0.00)	0.218 (± 0.02)	0.063 (± 0.001)
		B-6	40% + 60% HO	2.87 (± 0.13)	0.078^{e} (± 0.006)	2.5^{i} (± 0.1)	1.4^{b} (± 0.1)	0.013 (± 0.00)	0.112 (± 0.00)	0.047 (± 0.002)

[a, b, c, d, e, f, g, h, i, j, k, l] no statistical significant difference

All the origins of palm oil and all the blends have been studied with triplicate measures for crystallization studies and solid fat content and with quintuplicate measurments for oscillation rheology. Values in parenthesis represent confidence intervals ($\alpha = 0.05$). Parenthesis of the degree of rigidity *m*, by calculation of measurement failure

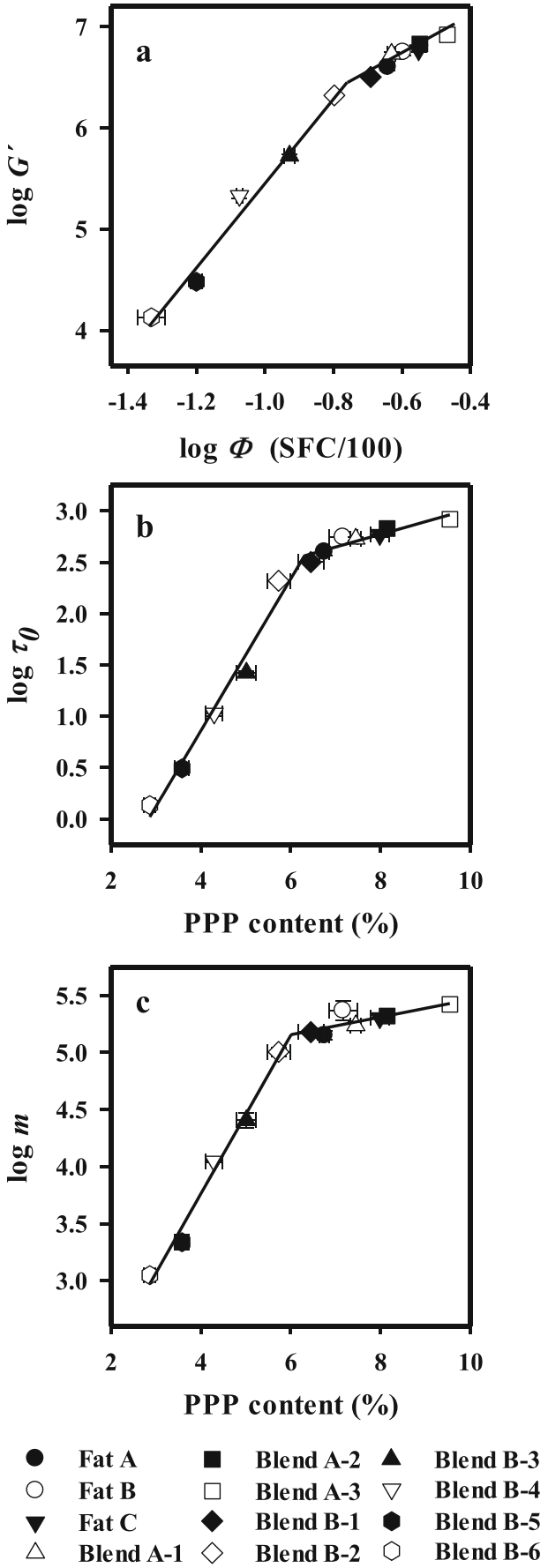

◀ **Fig. 4** **a** Elastic modulus at the stress at the limit of linearity (log G') as a function of the solids volume fraction (log Φ). **b** Stress at the limit of linearity (log τ_0) as a function of the tripalmitin (PPP) content (%). **c** Relationship of gel rigidity log $m(f)$ (= increasing elastic modulus G' with increasing frequency) of the respective fats as a function of their PPP content. Fat **A**: Ecuador; **B**: Ghana; **C**: Colombia, **A-1**: 5% palm stearin (PS); **A-2**: 10% PS; **A-3**: 20% PS, **B-1**:10% hazelnut oil (HO), **B-2**: 20% HO; **B-3**: 30% HO; **B-4**: 40% HO; **B-5**: 50% HO; **B-6**: 60% HO. Error bars represent confidence intervals ($\alpha = 0.05$) from amplitude and frequency sweeps from quintuplicate measures, and from triplicate measures of Φ taken by nuclear magnetic resonance spectroscopy; all solid fat content measurements taken at 20 °C

two different regions of mechanical response in Fig. 4 can be discerned when beginning to add hazelnut oil even at low concentrations, which would rationalize the disposition toward "oiling off" observed in Nougat cremes prepared from palm oil as the structuring agent.

The elastic properties of the fat crystal network increase with increasing addition of a PPP–rich fraction (see Fig. 4b and c, respectively). However, the increase in elastic properties follows a lower degree comprising the linear region with a flatter slope (see Fig. 4) of log G' versus Φ. This observation is coherent with other studies, showing that in a higher SFC region, elastic properties increase at a lower magnitude than in a lower SFC region [10, 37]. Explanations for this observation were given by Marangoni and Tang [37], who found that in higher SFC regions, more "dangling ends" are present in the crystalline network, which corresponds to solid fat particles not connected to neighboring clusters. Hence, such loose ends do not reinforce the stress-carrying solids and so do not contribute to the elastic properties of a network, even though Φ is increasing [37]. Thus, the increasing solids volume fractions Φ do not completely translate into more connections being formed. As a consequence, the elastic properties increase in the higher SFC region, yet at a lower extent compared with that in the low SFC region.

Crystallization Kinetics Studied by the Avrami Model and its Relation to the Solids Volume Fraction Φ and the Elastic Properties of the Fat Crystal Network

The two different linear regions for the maximum rate constants $k_g\ max$ as a function of the PPP content shown in Fig. 3 are mirrored in the relation of the elastic properties (log G') and the solids volume fraction corresponding to $k_g\ max$, as Fig. 5 displays. However, the course between the maximum rate constants $k_g\ max$ and the mechanical properties, surprisingly, appears to be mirror-inverted: (i) when viewing Fig. 3, $k_g\ max$ decreases at a lower descent by gradually increasing the hazelnut oil content, whereas, the elastic properties (via log G') show a rather sharp and dramatic decrease with increasing the hazelnut oil content (see Fig. 5). For example, by adding 40% hazelnut oil to Ghanaian palm oil (Fat B-4), the k_g

max expectedly dropped from 0.228 min^{-1} to not quite half the value (0.131 min^{-1}) while, concurrently, the mechanical properties, expressed as G' and gel rigidity m, decreased by 26- and 21-fold relative to the reduction of the speed of crystallization, respectively (see Table 3). (ii) Then, with the addition of a PPP-rich fraction, k_g *max* sharply increases, as displayed in Fig. 3; meanwhile, the elastic properties (log G') show a more moderate increase, as shown in Fig. 5.

When adding hazelnut oil to palm oil, the relationship between the crystallization kinetics, expressed as k_g *max*, and the elastic properties (G') seems to follow a power-law relationship ($R^2 = 0.996$). As discussed earlier in section 3.3., the elastic properties of colloidal gels and, thus, fat crystal networks depend on the stress-carrying solids volume fraction, which is strongly decreased by adding a liquid oil to a structuring fat, such as when hazelnut oil is mixed with palm oil. This behavior would explain the overproportionate loss of structure in comparison to the more discrete reduction of the rate constants when adding hazelnut oil to palm oil. From a crystallization kinetics standpoint, as indicated in Fig. 2, the higher melting fraction of palm oil in the blends with hazelnut oil still is readily crystallizing and thereby contributing to the determined values of k_g, in turn, clarifying the more discrete reduction of k_g *max*. Nonetheless, bulk crystallizable portions of the palm oil remain solubilized during crystallization (see Fig. 2) and, as the solids volume fraction Φ indicates, are largely kept solubilized during post-crystallization events. The drop in structural properties thereby uncouples from the linear correlation ($R^2 = 0.94$) between G' and k_g *max*, as shown for the palm oils of different geographical origins and the blends with palm stearin (see Fig. 5). These results demonstrate that by relatively small increases in k_g *max* (via increasing PPP content; see Figs. 3 and 4b, c), substantial benefits toward higher elastic properties can be achieved for mixtures of hazelnut oil with palm oil.

Avrami Exponents and their Relation to Elastic Properties of the Fat Crystal Network

As can be expected regarding the palm oils of different geographical origins, those with higher maximum rate constants k_g *max* (0.228 and 0.198 min^{-1} for Ghanaian and Colombian palm oil, respectively) also showed significantly higher elastic properties ($G' = 5.60$ and 5.86 MPa, and τ_0 = 559 and 588 Pa, respectively) when compared with those exhibited by the Ecuadorian palm oil, which displayed the lowest rate constants and elastic properties (k_g *max* = 0.130 min^{-1}, $G' = 4$ MPa, and τ_0 = 400 Pa; see Table 3). This observation can be fully attributed to differences in the composition of the TGs of the different origins of palm oil. For example, both the significantly higher content of U-U-U-type TG and the lower amount of Sat-Sat-Sat-type TG (see both in Table 2) in Ecuadorian palm oil translates into significantly lower rate constants. In turn, there is a lower bulk density (Φ) and, consequently, a lower connectivity of the network (expressed as a reduced elastic modulus G'), a reduced stress at the limit of linearity, and a lower τ_0 and gel rigidity m compared with the other two origins of palm oil.

The Avrami exponent n, related to the dimension of crystal growth, was similar between the palm oil origins having comparable values of k_g *max* ($n = 4.1$ and 4.0 for Ghanaian and Colombian palm oils, respectively) and different from Ecuadorian palm oil that crystallized at a lower rate (n = 3.6). Hence, similar crystallization properties (k and n) coincide with comparable elastic properties regarding the palm oils of different geographical origins, corroborating the findings of Singh et al. [17], who achieved two palm oil-based fats with similar mechanical properties to each other, by matching

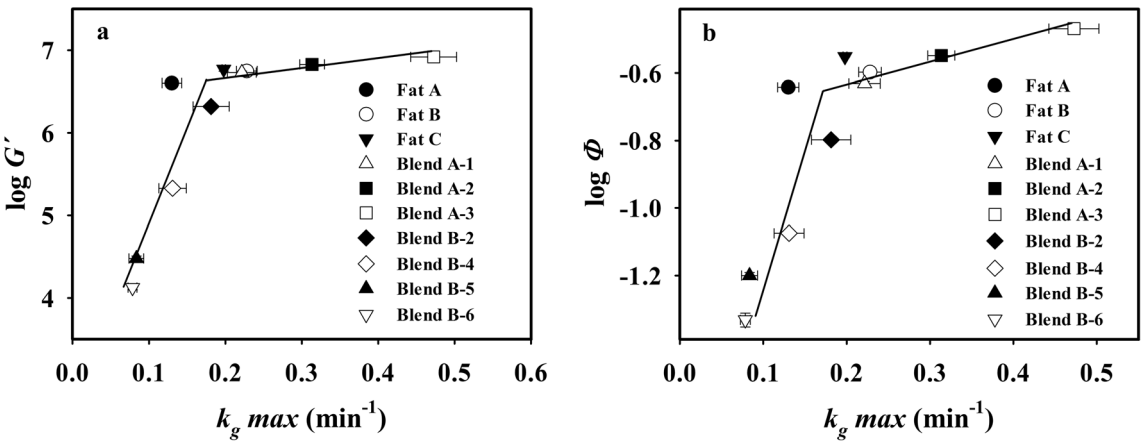

Fig. 5 **a** Elastic modulus at the stress at the limit of linearity (log G') as a function of the maximum rate constant k_g *max*; **b** log Φ as a function of k_g *max*, for palm oils of different geographic origins, Ghanaian palm oil and its dilutions with hazelnut oil (HO), and Ecuadorian palm oil blended with palm stearin (PS) as a tripalmitin-rich fraction. Fat **A**: Ecuador; **B**: Ghana; **C**: Colombia, **A-1**: 5% PS; **A-2**: 10% PS; **A-3**: 20% PS, **B-2**: 20% HO; **B-4**: 40% HO; **B-5**: 50% HO; **B-6**: 60% HO. Confidence intervals ($\alpha = 0.05$) for k_g *max* and Φ from triplicate and quintuplicate measures for G'

their Avrami exponents. However, limitations have to be considered when wanting to achieve similar mechanical properties by matching them with Avrami exponents alone. Regarding Ecuadorian palm oil, its Avrami exponent n increased with palm stearin addition in the first step when compared with unblended Ecuadorian palm oil. When adding 5% palm stearin, n significantly rose from 3.6 to 4.1, a value comparable to the palm oils of the other geographical origins, as were the elastic properties. However, values of n remained at levels around $n \approx 4$ when adding more palm stearin but the elastic properties further increased significantly (see Table 3). Hence, the Avrami exponent uncouples from the increase in elastic properties and cannot be harnessed as the sole measure to achieve a common hardness. This observation appears to be logical in the physical context of the Avrami exponent n, as it is only defined up to a crystal growth dimension of 4, whereas, values above 4 can be seen as artifactual [1]. Moreover, the Avrami exponent (n) can have the same value yet account for different types of crystal growth dimensions. For example, a plate-like growth from sporadic nuclei, or a spherulitic growth from instantaneous nuclei, are both described by an Avrami exponent $n = 3$ [1].

In the case of the dilution of Ghanaian palm oil with hazelnut oil, the Avrami exponent n significantly dropped with the increase in hazelnut oil, highlighting the relationship between elastic properties and crystal growth dimension [16, 18]. This trend is reinforced by the fact that two different fractal dimensions were displayed for the palm oils either blended with PPP or diluted with hazelnut oil in section 3.3 (see Fig. 4 and Eqs. 2 and 7). Our results highlight that the higher the addition of hazelnut oil, the lower the crystal growth dimension (Avrami exponent n) and the lower the elastic properties, as demonstrated in Fig. 6, and comprehensively shown in Table 3. When relating the solids volume fraction Φ of the dilutions of Ghanaian palm oil with hazelnut oil to the Avrami exponent n via Pearson's correlation, the correlation coefficient is 0.97 ($P = 0.007$). Hence, the solids content Φ is strongly and positively correlated with the different crystal types, shown by the crystal growth dimensions n, demonstrating that different crystal types are formed, depending on the solids content, as postulated earlier by Awad et al. [10].

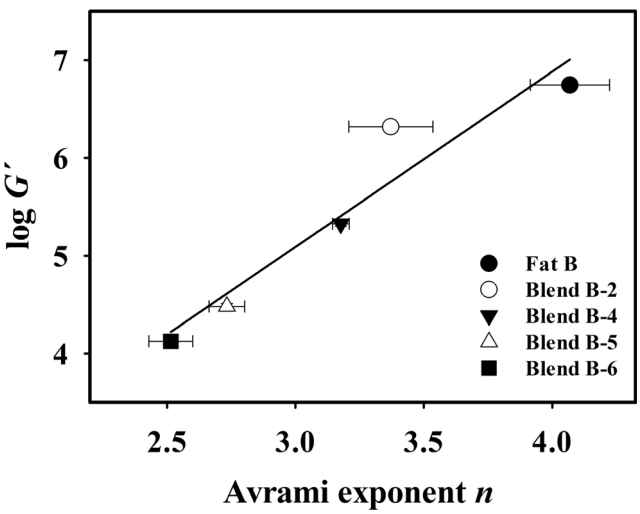

Fig. 6 Elastic modulus at the stress at the limit of linearity (log G') for Ghanaian palm oil diluted with hazelnut oil (HO) as a function of the Avrami exponent n corresponding with the maximum rate constants k_g *max*. $R^2 = 0.92$. Fat **B**: Ghana; **B-2**: 20% HO; **B-4**: 40% HO; **B-5**: 50% HO; **B-6**: 60% HO. Confidence intervals ($\alpha = 0.05$) for n from triplicate and quintuplicate measures for G'

Structural properties depend on or even result from the innate ability of fat to crystallize and the way its crystal network grows upon crystallization. The elasticity of fat crystal networks may depend on the solids volume fraction Φ (SFC/100) and appears to be strongly influenced by its interconnectivity. Adding small portions of liquid oil to a structuring fat does not necessarily lead to a strong decrease in crystallization properties, which would then generate soft fat crystal networks. Conversely, to a greater degree, the liquid oil strongly dilutes crystallizable portions of the structuring fat and changes the crystal growth dimension, which is expressed by a changed fractal dimension. As a result, the mechanical properties decrease in a power-law fashion upon the dilution with liquid oil.

Conclusion

This study further explored the recognized link between crystallization kinetics, the SFC (via the solids volume fraction Φ), and the resulting mechanical properties through combining results from an extended Avrami model [7] with oscillation rheology. The application of an extended Avrami model verified that the progression of the bell-shaped curves of the rate constants strongly depends on the lipid composition of the investigated oils, correlating well with fundamental physics on crystallization. In general, the relationship between crystallization kinetics and elastic properties has to be discerned between hazelnut oil addition and increasing PPP content by palm stearin addition since the gel rigidity and elastic properties of the materials follow two different rheological regions versus PPP content and Φ. In the lower SFC region, structural properties increase faster by an increasing solids volume fraction, and more slowly in a higher SFC region. Hazelnut oil presents a strong dilutive character on the crystallizable portions of the palm oil, notably on POP. In this way, the structural properties are over-proportionately reduced, as the interconnectedness between crystal aggregates appears to be strongly reduced. At the same time, rate constants did not follow this strong decrease, resulting in a power-law relationship between the rate constants and elastic properties for palm oil diluted with hazelnut oil. Moreover, the Avrami exponent n, representing the crystal growth dimension, had a strong

positive correlation with the resultant elastic properties. The lower the n, the lower the subsequent material strength for the mixtures of palm oil with hazelnut oil.

Thus, distinct associations between crystallization kinetics, the solids volume fraction of crystallized fat, and the resultant mechanical properties have been shown. Nonetheless, the interrelation between these parameters is more complex, as a mirror-inverted relation between the rate constants, related elastic properties, and Φ demonstrates. Rate constants increase moderately, the less hazelnut oil is added, but elastic properties increase in a power-law fashion. Rate constants sharply increase by the addition of PPP-rich fractions to palm oil, yet structural properties increase more moderately. At first sight, this may appear as a contradiction. Nonetheless, these findings offer some aspects to be considered by the producers of palm oil-based nougat cremes: Increasing the number of nuts in the recipe improves the taste and health properties alike, but it deteriorates the structural properties and the cremes disposition to show liquid oil separation at the surface. It was also shown that by minor increases in the PPP content of hazelnut–palm oil mixtures, huge structural gains are possible. Thus, by improving the crystallization properties of palm oil through the addition of a PPP-rich fraction, crystallization properties necessary for safe production and, notably, proper structural properties could be possibly acquired to avoid "oiling off" during later shelf storage. Thus, by its rather slow crystallization properties and its vulnerability toward solubilization in hazelnut oil, palm oil may be part of the problem, but it also offers a solution through its derived PPP-rich fractions. These proper attributes can be achieved without being necessarily at the cost of a good spreadability and a tender melt-in-mouth since further adjustments can be tailormade by the application of an extended Avrami model with oscillation rheology.

Summarizing the results, this study highlights the complexity and difficulty encountered when designing new recipes involving the addition of liquid oils. For example, adding liquid oil via nuts, even in low portions, has a tremendous impact on the elastic properties of the product and thereby its stability against "oiling off." This fact should be of high relevance to food manufacturers.

Acknowledgments We would like to thank the former company supervisor of Stephen-Sven Hubbes, Steffen Rapp, Head of the Quality Department of Rapunzel Naturkost GmbH, for launching this project. We also want to thank Rapunzel Naturkost GmbH for providing all the resources needed to conduct these studies and Thorsten Tybussek from the Fraunhofer IVV for HPLC analysis of the triglycerides and his scientific support in this project.

Funding This work was financed by Rapunzel Naturkost GmbH, Legau, Germany, www.rapunzel.de.

Compliance with Ethical Standards

Conflict of Interest The research was funded by Rapunzel Naturkost GmbH. Stephen-Sven Hubbes is Head of the Research & Development Department of Rapunzel Naturkost GmbH. André Braun works for Anton Paar Germany GmbH and was employed at the Technical University of Munich (TUM®) during the elaboration of this work.

References

1. A.G. Marangoni, L.H. Wesdorp, In Structure and Properties of Fat Crystal Networks, ed. By A.G. Marangoni, L.H. Wesdorp (CRC Press, Boca Raton, 2013) p. 27–99
2. S. Padar, S.A.K. Jeelani, E. Windhab, J. Am, Oil Chem. Soc. **85**(12), 1115–1126 (2008)
3. E. Dibildox-Alvarado, J.F. Toro-Vazquez, J. Am, Oil Chem. Soc. **75**(1), 73–76 (1998)
4. S.S. Narine, K.L. Humphrey, L. Bouzidi, J. Am Oil, Chem. Soc. **83**, 913–921 (2006)
5. G.M. de Oliveira, A.P.B. Ribeiro, O. dos Santos, L.P. Cardoso, T.G. Kieckbusch, LWT Food Sci. Technol. **63**, 1163–1170 (2015)
6. M. Avrami, J. Chem. Phys. **8**, 212–224 (1940)
7. S.S. Hubbes, W. Danzl, P. Foerst, LWT Food Sci. Technol. **93**, 189–196 (2018)
8. W.H. Shih, W.Y. Shih, S.I. Kim, J. Liu, I.A. Aksay, Phys. Rev. A **42**(8), 4772–4779 (1990)
9. A.G. Marangoni, N. Acevedo, F. Maleky, E. Co, F. Peyronel, G. Mazzanti, B. Quinn, D. Pink, Soft Matter **8**, 1275–1300 (2012)
10. T.S. Awad, M.A. Rogers, A.G. Marangoni, J. Phys. Chem. B **108**(1), 171–179 (2004)
11. M.A. Rogers, D. Tang, L. Ahmadi, A.G. Marangoni, In Food Material Science. Principles and Practice, ed. by J.M. Aguilera, P. Lillford, (Springer, New York, 2008), p. 369–414
12. D. Tang, A.G. Marangoni, J. Colloid Interface Sci. **318**(2), 202–209 (2008)
13. R. Vreeker, L.L. Hoekstra, D.C. den Boer, W.G.M. Agterof, Coll. Surfaces **65**(2-3), 185–189 (1992)
14. S.S. Narine, A.G. Marangoni, Phys. Rev. E **59**(2), 1908–1919 (1999)
15. A.G. Marangoni, M.A. Rogers, Appl. Phys. Lett. **82**(19), 3239–3241 (2003)
16. A.G. Marangoni, S.E. McGauley, Cryst. Growth Des. **3**(1), 95–108 (2003)
17. A.P. Singh, C. Bertoli, P.R. Rousset, A.G. Marangoni, J. Agric. Food Chem **52**(6), 1551–1557 (2004)
18. D. Pérez-Martínez, C. Alvarez-Salas, J.A. Morales-Rueda, J.F. Toro-Vazquez, M. Charó-Alonso, E. Dibildox-Alvarado, J. Am. Oil Chem. Soc **82**(7), 471–479 (2005)
19. M.A. Stahl, M.H.M. Buscato, R. Grimaldi, L.P. Cardoso, A.P.B. Ribeiro, LWT Food Sci. Technol **54**, 3391–3403 (2017)
20. M.A. Stahl, M.H.M. Buscato, R. Grimaldi, L.P. Cardoso, A.P.B. Ribeiro, Food Res. Int. **107**, 61–72 (2018)
21. K.M. Barbosa, L.P. Cardoso, A.P.B. Ribeiro, T.G. Kieckbusch, M.H.M. Buscato, J. Food Sci. Technol **55**, 1004–1115 (2018)
22. R. Boistelle, in Crystallization and Polymorphism of Fats and Fatty Acids, ed. by N. Garti, K. Sato, (Marcel Dekker, New York, 1989) p. 189–226
23. T. Mezger, in The Rheology Handbook, ed. by T. Mezger (Vincentz Network, Hannover, 2014), p. 159–176
24. M.F. Peyronel, A.G. Marangoni, Pulsed Nuclear Magnetic Resonance Spectrometry (AOCS Lipid Library 2018), http://lipidlibrary.aocs.org/Biochemistry/content.cfm?ItemNumber=40797#pulsed. Accessed 3 Dec 2018
25. S. Braipson-Danthin, V. Gibon, Eur. J. Lipid Sci. Technol. **109**(4), 359–372 (2007)

26. Z. Omar, N.A. Rashid, S.H.M. Fauzi, Z. Shahrim, A.G. Marangoni, LWT Food Sci. Technol. **64**, 483–489 (2015)
27. E. Yilmaz, M. Öğütcü, J. Am. Oil Chem. Soc **91**(6), 1007–1017 (2014)
28. K. Mondal, B.S. Murty, J. Non-Crystalline Solids **352**(50-51), 5257–5264 (2006)
29. R. West, D. Rousseau, Food Res. Int. **85**, 224–234 (2016)
30. K. Sangwal, K. Sato, in Structure–Function Analysis of Edible Fats, ed. by A.G. Marangoni (AOCS Press, Urbana, 2012) p. 25–78
31. K.W. Smith, K. Bhaggan, G. Talbot, K.F. van Malssen, J. Am, Oil Chem. Soc. **88**(8), 1085–1101 (2011)
32. R.W. Hartel, Annu. Rev. Food Sci. Technol. **4**(1), 277–292 (2013)
33. G. Calliauw, E. Fredrick, V. Gibon, W. De Greyt, J. Wouters, I. Foubert, K. Dewettinck, Food Res. Int. **43**(4), 972–981 (2010)
34. T. Okawachi, N. Sagi, H. Mori, J. Am. Oil Chem. Soc **62**(2), 421–425 (1985)
35. J. Vereecken, I. Foubert, K.W. Smith, K. Dewettinck, Eur. J. Lipid Sci. Technol. **111**(3), 243–258 (2009)
36. D. Tang, A.G. Marangoni, Trends Food Sci. Technol. **18**(9), 474–483 (2007)
37. A.G. Marangoni, D. Tang, Food Biophys. **3**(2), 113–119 (2008)
38. L. Duffours, T. Woignier, J. Phalippou, J. Non-Crystalline Solids **186**, 321–327 (1995)